

A Study of Resorption of the Hydroxyapatite in the Composition of Impregnated Carbon Implants

N. I. Ponomareva^a, T. D. Poprygina^a, Yu. A. Ponomarev^b, and S. A. Soldatenko^b

^a Burdenko Voronezh State Medical Academy, ul. Studencheskaya, 10, Voronezh, 394000 Russia
e-mail: tanechkavma@yandex.ru

^b Voronezh State University, Voronezh, Russia

Received July 21, 2011

Abstract—Experimental data on the resorption of hydroxyapatite from the impregnated carbon implants as a dependence on the crystal composition, size and morphology are presented. It was proved using XRD, IRS, LRSMA, TEM, SEM, and gravimetry that the hydroxyapatite nanocrystals not contaminated by impurity phases exhibited the minimum resorption in the acidic environment.

DOI: 10.1134/S1070363212090022

Constantly growing interest in hydroxyapatite $\text{Ca}_{10}(\text{PO}_4)_6(\text{OH})_2$, the main inorganic component of bone tissue, is due to its potential use in reparative medicine. There are ceramic materials, cements, pastes, suspensions, and coatings based on this calcium hydroxyapatite. A numerous reviews [1–7] discussed in detail shortcomings and advantages of these forms. For example, the fragility of bioceramic substantially restricts its use in trauma treatment, where still the most popular is the use of metal structures and carbon implants that meet all the requirements of strength, but unfortunately, have no the desired biological activity. The use of the protein growth factors of bone tissue and hydroxyapatite as a filler of carbon-carbon implants presents a significant opportunity of reviving the inert material of the matrices in reconstructive surgery [8]. Therefore a study is of interest of resorption of crystals of a certain composition, size and morphology from the pores of the impregnated implant at the pH of blood (7.4 ± 0.05), as well as at the pH produced by the osteoclasts, the cells of destroyers ($\text{pH} \geq 4$). The purpose of this paper is to investigate the very possibility of impregnating the carbon implants with hydroxyapatite obtained in various ways, as well as the study of resorption of these materials in the slightly alkaline or acidic environment.

We found that in the implants immersed in aqueous or non-aqueous solution during the synthesis of hydroxyapatite additional phases are formed. In the diffractograms (Fig. 1) usually the high intensity peaks

occur at $d = 3.21, 2.88, 2.61, 1.94, 1.73 \text{ \AA}$, corresponding to $\beta\text{-Ca}_3(\text{PO}_4)_2$, the material possibly includes CaCO_3 (the main line corresponds to the interplanar spacing $d = 3.035 \text{ \AA}$), and a phase of $\beta\text{-Ca}_2\text{P}_2\text{O}_7$ [reflexes at $d = 3.23, 3.08, 3.04, 2.76 \text{ \AA}$ superimposed in part with the lines of the hydroxyapatite or $\beta\text{-Ca}_3(\text{PO}_4)_2$].

This fact is due apparently to the uneven distribution of the reactants in the implant pores during the synthesis of hydroxyapatite, as well as by local variations of pH in the pores. The pore size is about 500 \mu m . In the SEM-micrographs the presence is seen of a mixture of spherical, lamellar, and needle-like aggregates. According to elemental analysis (LRSMA) the Ca:P molar ratio is 1.63.

A forced impregnation of the material with the freshly prepared aqueous solution of hydroxyapatite led to better results: the phase composition of the samples did not change, the Ca:P molar ratio was 1.67, and the hydroxyapatite formed a uniform adsorption layer of spherical particles of size less than 100 nm . At keeping the samples in the corresponding aqueous solutions, the surface morphology changed: the size of the aggregates of the hydrated particles reaches 5 \mu m . Figure 2 shows the appearance of the implants.

The microemulsion method followed by annealing at 400°C led to formation of the nanosized particles (about 30 nm) in the implant pores. The sample had a crystalline structure and was identified as a hydroxy-

apatite doped with other calcium phosphate phases and an amorphous phase (the Ca:P molar ratio is 1.78). As in the case of deposition of hydroxyapatite in an aqueous medium, the presence of the implant in the emulsion from the beginning of synthesis showed the worst results, may be due to the uneven distribution of the reagents which are forced to diffuse into the implant pores. The TEM method revealed that in solution the particles have anisotropic shape (length and width are 10–20 and 2–4 nm, respectively), and are coated with an amorphous shell (Fig. 3).

Rather interesting results were obtained at growing the hydroxyapatite crystals by alternately changing solutions of calcium nitrate and ammonium hydrogen phosphate in an alkaline environment. The lamellar crystals formed are of 100–500 μ size and form tufts on the surface of the implant carbon fibers. A typical diffraction pattern allowed us to determine the characteristic interplanar spacings ($d = 3.44, 2.82, 2.78, 2.72, 2.63, 2.26, 1.94, 1.84$ Å) if the hydroxyapatite not contaminated with other phases. The IR spectra contain the bands of stretching and bending vibrations of phosphate groups with $\nu(\text{PO}_4^{3-})$ 1048, 604, 567 cm^{-1} , free hydroxy groups at $\nu(\text{OH})$ 3622 cm^{-1} , and the hydroxy groups associated by intermolecular hydrogen bonds, at 3427 cm^{-1} .

To consider the results obtained at testing the samples for resorption, we classify series of impregnated implants as follows: series no. 1, the implant saturated with hydroxyapatite contaminated with other phases of the precursor [$\text{Ca}_3(\text{PO}_4)_2$, $\text{Ca}_2\text{P}_2\text{O}_7$, CaCO_3 , etc.], appearing at immersing the implant in the solution at the synthesis beginning, ratio Ca:P = 1.63; series no. 2, the implant filled with hydroxyapatite obtained in an aqueous solution by the nitrate method, ratio Ca:P = 1.67; series no. 3, the implant filled with hydroxyapatite obtained by the microemulsion method. Ratio Ca:P = 1.78.

The adsorption from the series no. 1 was 38.3–38.5 mg g^{-1} , impregnation of samples in the 2nd and 3rd series resulted in the adsorption of 21.0–24.0 mg g^{-1} of hydroxyapatite in the carbon implant.

At keeping a sample in a solution with pH of 7.35 the relative loss of the implant weight ($\Delta m \times 100\%/m$) was 0.11–0.18% in all series. Hence, in a weakly alkaline medium the hydroxyapatite filler is stable and the results may serve as a reference for comparison with other experimental data.

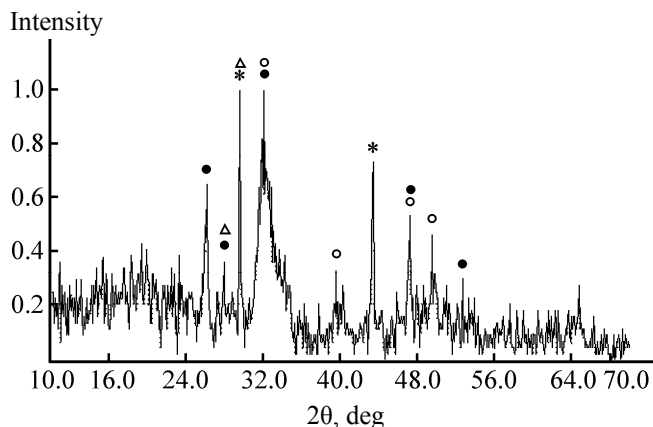


Fig. 1. Diffractogram of hydroxyapatite containing the impurity phases: $\beta\text{-Ca}_3(\text{PO}_4)_2$ (dark circles), hydroxyapatite (clear circles), $\text{Ca}_2\text{P}_2\text{O}_7$ (triangles), and CaCO_3 (asterics).

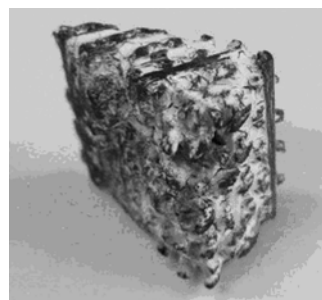


Fig. 2. Photograph of the implant impregnated with hydroxyapatite obtained in aqueous solution.

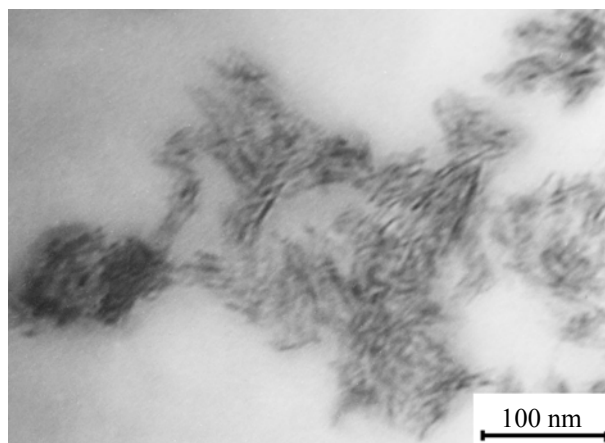


Fig. 3. Brightfield TEM image of hydroxyapatite obtained by microemulsion method.

The results of testing resorption at pH 6.0 are shown in Fig. 4. The weight loss reaches its maximum value (2.15%) in the samples of the 1st series, the series nos. 2 and 3 both showed resorption reaching its maximum 1.15% on the third day (4320 min) of keeping the samples in the corresponding solutions. In

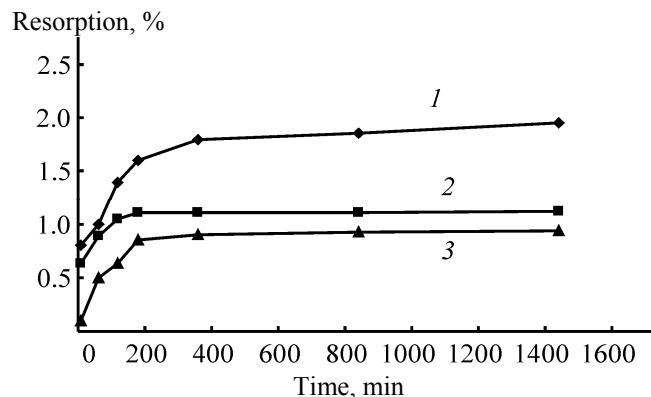


Fig. 4. Resorption (relative weight loss) of hydroxyapatite at pH 6.0, the curve numbers correspond to the numbers of the series.

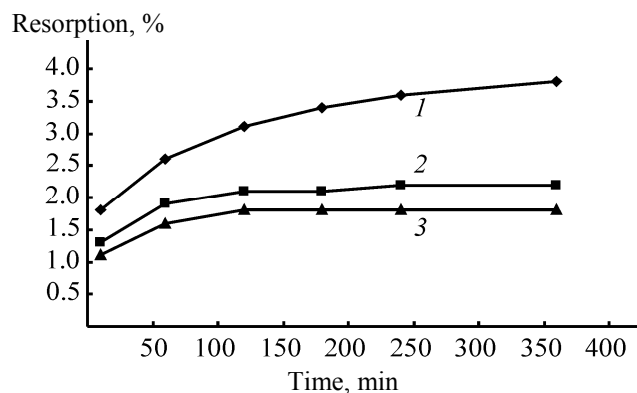


Fig. 5. Resorption of hydroxyapatite at pH 4.0, the curve numbers correspond to the numbers of the series.

addition, the samples of the series no. 1 showed a tendency to further increase in the resorption.

The increase in the acidity to pH 4.0 resulted in an increased resorption, which again reached a maximum (3.8%) for the samples of series 1 in 6 h of keeping the implants in the solution. The corresponding values for samples of 2-nd and 3-rd series were 2.2 and 1.8% (Fig. 5). As in the previous case, the series no. 1 showed a tendency to further increase in the resorption. Table 1 lists some characteristics and the results of testing the materials.

A comparison of the implants after forced impregnation with those coated with the hydroxyapatite crystals grown *in situ* also revealed a significant difference in resorption despite of the same molar ratio Ca:P = 1.67. The maximum resorption from the grown crystals was 2–2.5 times higher than the resorption from the artificially applied hydroxyapatite. This obviously is connected with the difference in the size and morphology of the particles.

Thus, the results of the tests led us to the following conclusions. The hydroxyapatite contaminated with other phases [$\text{Ca}_3(\text{PO}_4)_2$, $\text{Ca}_2\text{P}_2\text{O}_7$, and CaCO_3] penetrates

easier in the pores of the implant carbon matrix, resulting in an increased adsorption, but the multiphase filler showed also an increased resorption in acidic solutions, so the implants should not be immersed in the solution at the synthesis of hydroxyapatite. For the impregnation of carbon implants with hydroxyapatite we recommend to use the microemulsion method followed by annealing at 400°C, which allows obtaining the nano-sized particles in the implant pores, or an aqueous synthesis using concentrations no higher than 0.1 M with the dropwise addition of the phosphate solution to that of calcium salt. Both methods give satisfactory results in terms of resorption *in vitro*. In addition to the phase composition, the size of the crystals affects the hydroxyapatite resorption: the resorption from the material containing crystals of smaller size is found to be lower at the same molar ratio Ca:P = 1.67.

Table 2 shows advantages and disadvantages of the methods of various ways of introducing the hydroxyapatite to the matrix pores.

EXPERIMENTAL

We used the material for implants comprising carbon fibers bound in a single block of carbon matrix.

Table 1. Features of the implants impregnated with hydroxyapatite

Series	Adsorption by the implant matrix, mg g ⁻¹	Ca:P molar ratio	Particle size, nm	Maximum resorption, % at pH = 6.0	Maximum resorption, % at pH = 4.0
1	38.4±0.1	1.63	100–2000	2.15	3.8
2	23.0±1.0	1.67	80–100	1.15	2.2
3	22.0±1.0	1.78	30–50	1.15	1.8

Table 2. Advantages and disadvantages of the samples of studied series

Method no.	Advantages	Disadvantages
1	Increased adsorption	Nonuniform phase composition, enhanced resorption
2	Absence of admixtures, stoichiometric composition of the substance, decreased resorption	Increased degree of hydration and the larger particles size
3	Decrease in the particle size, decreased resorption	Increased synthesis duration, necessity of thermal treatment

The implants are thermally stable (up to 3500°C), conductive, with the compressive strength above 40 MPa, the bend strength above 20 MPa, the elasticity modulus above 29 GPa, the pore size 500 μ , the total porosity 11–22 vol %, open porosity 6–15 vol %. Thus, in contrast to bioceramics, the carbon matrix implants have mechanical properties corresponding to those of the bone tissue, and porosity sufficient for the germination of the newly formed bone tissue through the structure of the carbon-carbon implant.

The hydroxyapatite was prepared by aqueous [9] and microemulsion [10] methods.

We performed the natural and forced impregnation of the implants with the hydroxyapatite. At the natural impregnation the implant was immersed in the solution at the synthesis of hydroxyapatite or was heated in a suspension of freshly prepared hydroxyapatite followed by evaporation. At the forced impregnation the hydroxyapatite suspension was injected into the pores of the implant with a syringe. Separately the growth of the hydroxyapatite crystals on the implant fibers was investigated: the implant was alternately placed in the solutions of calcium nitrate and ammonium hydrogen phosphate every 2 days, maintaining pH 10 with ammonia. In all cases, the samples were dried at room temperature.

Electron microscopy (SEM) was carried out on a JSM-6380 LV instrument (Japan), local X-ray spectral microanalysis (LRSMA) was performed using an Energy-250 setup. Infrared spectra in the range 4000–400 cm^{-1} were taken on infrared spectrometers Infracum FT-02 and Specord IR-75, the samples were compressed into tablets with KBr. The diffraction

patterns were obtained on a DRON-3M and a DRON-7 devices, $\text{CuK}\alpha$ radiation, scan rate 2 deg min^{-1} . The shape, size (particle size distribution) and the structure of the particles were determined from the data of a high-voltage transmission electron microscopy (TEM) obtained with the electron microscope EMW-100BR. The analyzed material was dispersed in water with ultrasound and the dispersed powder was applied to a carbon substrate.

REFERENCES

1. Barinov, S.M. and Komlev, V.S., *Biokeramika na osnove fosfatov kal'tsiya* (Bioceramic Based on Calcium Phosphate), Moscow: Nauka, 2005.
2. Putlyayev, V.I., *Sorovskii Obrazovatel'nyi Zh.*, 2004, vol. 8, no. 1, p. 44.
3. Kalkura, S.N., Anee, T.K., Ashok, M., and Betzee, C., *Bio-Med. Mater. Eng.*, 2004, no. 14, p. 581.
4. Zakharov, N.A. and Orlovskii, V.P., *Materialovedenie*, 2002, no. 8, p. 22.
5. *Biomaterials Science: An Introduction to Materials in Medicine*, Ratner, B.D., Ed., San Diego: Academic Press, 1996, p. 82.
6. Hench, L., *J. Am. Ceram. Soc.*, 1991, vol.74, no. 7, p. 1487.
7. Shpak, A.P., Karbovskii, V.L., and Trachevskii, V.V., *Apatity* (Apatites), Akademperiodika, 2002.
8. Burlakov, S.V., *Candidate Sci. (Chem.) Dissertation*, St. Petersburg, 2009.
9. Ponomareva, N.I., Poprygina, T.D., Lesovoi, M.V., and Karpov, S.I., *Zh. Obshch. Khim.*, 2008, vol. 78, no. 4, p. 538.
10. Ponomareva, N.I., Poprygina, T.D., Karpov, S.I., Lesovoi, M.V., and Agapov, B.L., *Zh. Obshch. Khim.*, 2010, vol. 80, no. 5, p. 735.